First-principles study of the elastic constants and optical properties of uranium metal*

Chen Qiu-Yun(陈秋云)†, Tan Shi-Yong(谭世勇),
Lai Xin-Chun(赖新春), and Chen Jun(陈 军)

Science and Technology on Surface Physics and Chemistry Laboratory, Mianyang 621907, *China*

(Received 15 December 2011; revised manuscript received 6 January 2012)

We perform first-principles calculations of the lattice constants, elastic constants, and optical properties for alpha- and gamma-uranium based on the ultra-soft pseudopotential method. Lattice constants and equilibrium atomic volume are consistent pretty well with the experimental results. Some difference exists between our calculated elastic constants and the experimental data. Based on the satisfactory ground state electronic structure calculations, the optical conductivity, dielectric function, refractive index, and extinction coefficients are also obtained. These calculated optical properties are compared with our results and other published experimental data.

Keywords: uranium, electronic structure, elastic constants, optical properties

PACS: 78.20.Ci, 71.20.Gj, 71.27.+a **DOI:** 10.1088/1674-1056/21/8/087801

1. Introduction

Uranium, the heaviest naturally occurring element, has received a lot of attention for its nuclear properties and potential applications in nuclear power and the nuclear weapon industry. Its physical and chemical properties are constantly of great interest to scientists , and are largely determined by its electrons surrounding the nuclei, especially the 5f electrons, in the solid. Interesting properties of uranium include low temperature charge-density wave (CDW) transition, anisotropic thermal expansion, and a relatively complex crystal structure (orthorhombic). Recent analysis shows that uranium is also a promising material for mirror coatings in the soft X-ray range and the extreme ultra-violet (EUV) region, and that uranium thin films can be used in space telescopes and in multilayer mirrors.[1,2] Also, in nuclear industry, in order to evaluate the extent of oxidation for the surface, it is necessary to obtain the thickness of the oxide layer. For some conventional thickness-determination techniques like ellipsometric spectroscopy, optical constants such as refractive indices and extinction coefficients are the necessary parameters. Exploring the optical properties of uranium is of great importance both in technological and in application aspects.

As regards the optical properties of uranium, experimentally the optical properties of uranium and its oxide have been studied since the early 1990s by different research teams.[3−8] Optical properties of evaporated films of uranium were studied for the first time by Faldt and Nilsson[6] in a range of 0.6 eV–25 eV. Optical conductivity was obtained from a combination of the ellipsometric measurements (0.6 eV–4.1 eV) and the normal incidence reflectance measurements (3 eV–25 eV). Optical constants n (refractive index) and k (extinction coefficient) at a fixed wavelength of 546.1 nm have been obtained by Ritchie[9] to be $n = 3.1$ and $k = 3.9$ for uranium, and $n = 2.2$ and $k = 0.5$ for the oxide grown on a uranium substrate. Wide band (200 nm–900 nm) ellipsometric measurements for a polished uranium surface and its epitaxial oxide were performed by Siekhaus *et al.*[7] for the first time. Theoretically, although there are some papers dealing with the optical properties of certain new materials,[10−15] only a few papers dealt with the optical properties of uranium. Gasche *et al.*[16] calculated the optical conductivity of uranium using a linear muffin-tin orbital method in the density functional theory. Exploring the electronic structure and optical properties of uranium should have great significance for extending the range of practical applications. Furthermore, it can provide interpretations for experimental data.

Solid uranium has alpha (orthorhombic)-, beta (tetragonal)-, and gamma (body centered cubic)-

*Project supported by the National Natural Science Foundation of China (Grant No. 91026016).
†Corresponding author. E-mail: sheqiuyun@126.com
© 2012 Chinese Physical Society and IOP Publishing Ltd

phases, and which phase is present depends on temperature and pressure. The α–U can exist at room temperature and ambient pressure, and it can be stabilized into the gamma phase when another element is added (Ti, Nb, etc.). Both α–U and γ–U transition metal alloys have been used widely in nuclear reactors, and are of great importance in the nuclear weapon industry. Their physical and chemical properties are constantly of great interest to scientists. Exploring both ground state and optical properties of these two phases is important.

Wills and Eriksson[17] used the local density approximation (LDA) to perform the density-functional and full-potential calculations, in which the correct ground-state structure of uranium could be reproduced, but the equilibrium volume was not very well described. A few years later the LDA was replaced by a generalized gradient approximation (GGA) treatment of the electron exchange–correlation functional,[18] and the equilibrium volume was in much better agreement with the experimental results. Since then, several theoretical investigations of the equilibrium volumes in the actinides have been published, and a summary was given in the paper by Jones *et al.*[19] The electronic structure of uranium is dominated by 5f electron states which form bands that are very narrow and tend to bond the atoms in complex and distorted ways.[20] The combination of narrow 5f states and an open distorted crystal structure make a theoretical treatment nontrivial. In the following we use a pseudopotential method and GGA as the exchange–correlation functional to explore the ground state properties of uranium. Moreover, we will investigate the elastic constants of both α–U and γ–U. According to our survey, elastic properties of uranium have been calculated only by Söderlind[21] using the full-potential method and by Taylor[22] using the projector augmented-wave (PAW) technique. The determination of elastic constants is important because they contain detailed information about chemical bonds and provide a very sensitive test of the theory.

The rest of the present paper is organized as follows. In Section 2, we describe theoretical details of our method, including typical parameters set for the calculations. In Section 3, we optimize the structure of uranium, elastic constants, and optical properties of α–U and γ–U. Finally in Section 4, a conclusion is made and also future prospects are given.

2. Computational details

The results described below are based on the density function theory, as implemented in CASTEP code, in which is used a plane wave basis set for expansion of effective single particle Kohn–Sham energy.[23,24] Ultra-soft pseudo-potentials are used to describe the interactions between the ionic core and valence electrons. The exchange–correlation functional is a GGA of Perdew–Burke–Ernzerhof (PBE) formalism.[25] The pseudopotential approximation replaces core electrons and the strong Coulomb potential by a weaker pseudopotential that acts on a set of pseudowavefunctions. This potential can be represented with only a small number of Fourier coefficients. Ultrasoft pseudopotentials (USP) were introduced by Vanderbilt (1990)[26] in order to allow calculations to be performed with the lowest possible cutoff energy for the plane-wave basis set. In the ultrasoft pseudopotential scheme the pseudo-wave-functions are allowed to be as soft as possible within the core region, so that the cutoff energy can be dramatically reduced. The total energy in the USP scheme has the same form as those in other pseudopotential plane-wave methods, with the nonlocal potential $V_{\rm NL}$ given as

$$V_{\rm NL} = \sum_{nm,I} D^{(0)}_{nm} \left|\beta^I_n\right\rangle \left\langle\beta^I_m\right|, \tag{1}$$

where the projector β and coefficient $D^{(0)}$ characterize the pseudopotential and are different for different atomic species. The index I refers to the atomic site. The electron density in the expression for the total energy is given by

$$n(r) = \sum_i \left[|\phi_i(r)|^2 + \sum_{nm,I} Q^I_{nm}(r)\langle\phi_i|\beta^I_n\rangle\langle\beta^I_m|\phi_i\rangle\right], \tag{2}$$

where $\phi_i(r)$ are the wavefunctions and Q_{nm} are the augmentation functions that are strictly localized in the core regions. The ultrasoft potential is fully determined by the local part, $V^{\rm ion}_{\rm loc}(r)$ and by the coefficients $D^{(0)}$, Q, and β. Kohn–Sham equations can be rewritten for the USP case as

$$H\left|\phi_i\right\rangle = \varepsilon_i S\left|\phi_i\right\rangle, \tag{3}$$

where $S = 1 + \sum_{nm,I} q_{nm}\left|\beta^I_n\right\rangle\left\langle\beta^I_m\right|$, H can be presented as a sum of kinetic energy and local potential

$$H = T + V_{\rm eff} + \sum_{nm,I} D^I_{nm}\left|\beta^I_n\right\rangle\left\langle\beta^I_m\right|, \tag{4}$$

with $V_{\rm eff}$ containing $V^{\rm ion}_{\rm loc}(r)$, Hartree, and exchange–correlation terms. All the terms arising from the augmented part of the electron density are grouped with

the nonlocal part of the pseudopotential by defining new coefficients

$$D_{nm}^{I} = D_{nm}^{(0)} + \int \mathrm{d}r V_{\mathrm{eff}}(r) Q_{nm}^{I}(r). \quad (5)$$

Further technical details of the USP implementation, including expressions for the derivatives of the total energy can be found in Ref. [27] by Laasonen *et al.*

The α–U can be described as the orthorhombic structure, depending on the crystallographic definition of the space group *Cm-cm* (No. 63), and γ–U belongs to the space group *Im*-3*m* (No. 229) with the body-centred cubic (bcc) structure. Experimental lattice constants are $a = 2.836$ Å (1 Å=0.1 nm), $b = 5.867$ Å, and $c = 4.936$ Å for α–U; and $a = b = c = 3.467$ Å for γ–U, and they are used as the original parameters for our calculation. The 5f, 6s, 6p, 6d, and 7s electrons of U are explicitly treated as valence electrons. The electron wave function is expanded in plane waves up to a cutoff energy of 700 eV for both of them. Energy calculations in the first irreducible Brillouin zone are performed using a special k-point sampling method of the Monkhorst–Pack scheme, and 18×8×10 and 15×15×15 grids are adopted for α–U and γ–U, respectively. The Broyden–Fletcher–Goldhaber–Shanno (BFGS) optimization method[28] is used to find the ground state of the crystals in which both the atom positions and lattice parameters are optimized simultaneously. Total energy changes finally reduce to less than 2×10^{-6} eV/atom, and Hellman–Feynman forces acting on atoms are converged to less than 0.01 eV/Å, 0.02 GPa for stress and 5×10^{-4} Å for displacement, respectively. In order to obtain the accurate crystal structures and total energies, all structural degrees of freedom including unit-cell volume and shape as well as atomic positions are relaxed simultaneously.

3. Results and discussion

3.1. Crystal structure

Before calculating the elastic constants and optical properties of uranium, which is the main purpose of this paper, we try to determine the fully relaxed structure and density of states of the metal. The optimized lattice constants and equilibrium atomic volume are presented in Table 1.

Table 1. Lattice constants (in Å) and equilibrium volume (in Å^3) for crystalline phases of α–U and γ–U using the ultrasoft pseudopotential method, compared with the results of the projector augmented-wave (PAW) method by Taylor,[22] the full-potential calculations by Söderlind,[21] the pseudopotential calculations by Crocombette,[29] and experiment (50 K).[30]

	Our work	PAW	Full-potential	Pseudopotential	Expt.
			α–uranium		
a	2.826	2.800	2.845	2.809	2.836
b	5.906	5.896	5.818	5.447	5.867
c	4.891	4.893	4.996	4.964	4.936
Volume/atom	20.408	20.194	20.674	19.026	20.535
			γ–uranium		
a	3.46	3.43	3.46	3.37	3.47
Volume/atom	20.72	20.18	20.71	19.14	20.89

Our calculated lattice constants and equilibrium atomic volume for the bcc phase are a little smaller than the experimental one, but the results accord best with the experimental results among the results obtained from other methods. Also for the orthorhombic phase, only the calculated volume by the full-potential method is larger than the experimental one, whereas the other three methods all underestimate the volume. Our calculated results also accord very well with the experimental ones.

3.2. Elastic constants

The elastic constants of a material describe its responses to an applied stress or, conversely, the stress required to maintain a given deformation. Both stress and strain have three tensile and three shear components, giving six components in total. Any symmetry present in the structure may make some of these components equal and others may be fixed at zero. Thus, for γ–U it has only three different symmetry elements (c_{11}, c_{12}, and c_{44}); while for α–U it has nine independent elastic constants. Our calculated results are listed in Table 2.

Table 2. Elastic constants and bulk moduli for both α–U and γ–U, obtained with the projector-augmented wave (PAW) method by Taylor,[22] the full-potential calculations by Söderlind,[21] the pseudopotential calculations by Crocombette,[29] and in experiment (298 K).[31] "Expt. $T = 0$" refers to data obtained from a linear extrapolation of experimental elastic constants to those at $T = 0$ K.

	Our work	PAW	Full-potential	Pseudopotential	Expt.	Expt. ($T = 0$)
			α–uranium			
c_{11}	255	296	300		215	210
c_{22}	200	216	220		199	215
c_{33}	345	367	320		267	297
c_{12}	53	60	50		46	
c_{13}	45	29	5		22	
c_{23}	136	141	110		108	
c_{44}	127	153	150		124	145
c_{55}	115	129	93		73	95
c_{66}	88	99	120		74	87
B	132	149	130	182	115	
			γ–uranium			
c_{11}	101	161				
c_{12}	45	184				
c_{44}	138	56				
B	166	176		170		

In Table 2, we summarize our calculated elastic constants and compare with the experimental data. The experimental data are denoted as "Expt." In the table, room temperature data are from Fisher and McSkimin.[31] The temperature dependence of the elastic constant of uranium is rather strong, and Söderlind[21] found that with the exception of c_{11} which is nearly constant, c_{ii} increases linearly with temperature increasing from about 100 K to about 50 K at which the CDW transitions take place. To best compare theoretical zero-temperature data with experimental results, he did a linear extrapolation of c_{ii} from 100 K to zero, and the data obtained are denoted as "Expt. ($T = 0$)" in Table 2. For c_{ij} no such a temperature variation is measured and no extrapolation is therefore made. Almost all theoretical methods give higher elastic constants than experimental evaluations made at 298 K except c_{13} within the full-potential method. Impurity effects on the elastic constants are unknown and may possibly play a part in this discrepancy also. However our calculated elastic constants c_{22} and c_{44} are in surprisingly good agreement with the experimental ones, and c_{66} is very close to the experimental one when it is extrapolated to $T = 0$ K. Our calculated bulk modulus for α–U is consistent with that of the full-potential method.

3.3. Electronic structure

Since the optical spectra are directly calculated from interband transitions, an accurate description of the electronic structure is indispensable. In Söderlind's research, he found that the spin–orbit coupling effect could be of great importance for Np and Pu, but it has small influence on uranium.[21] In the following sections, the spin–orbit interaction (SOI) effect is not considered. In Figs. 1 and 2, we present total and partial densities of states (DOS) for α–U and γ–U, respectively. The density of states for γ–U is somewhat different from that of α–U. In both cases, the narrow bands located approximately between -2 eV and $+4$ eV are due mainly to the uranium 5f orbitals.

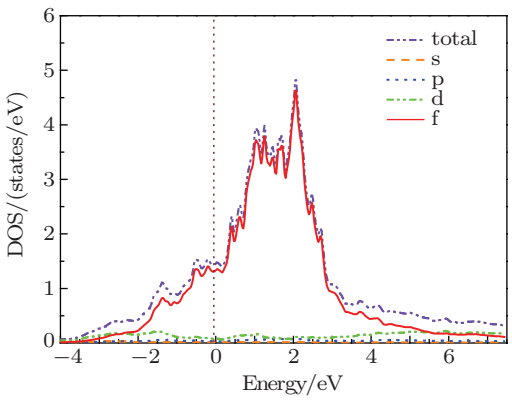


Fig. 1. (colour online) Total and partial densities of states (DOS) for α–U at the theoretical equilibrium atomic volume 20.41 Å^3. The Fermi level is set to be zero.

It also shows that the density of states for γ–uranium is split into more peaks than for α–U. For α–U we can see five sets of peaks, which consist of the f orbital

crystal field splittings. As we move to lower energies (away from E_F), among the occupied states the metallic d bands have comparable intensity to f bands. Note that above the Fermi level, showing the unoccupied states, there is a substantial difference between the two phases. The bcc structure has a peak at about 4 eV.

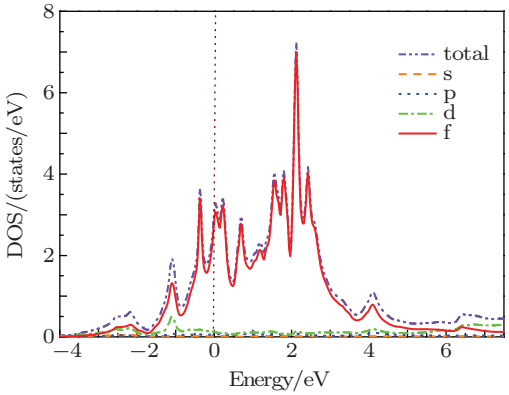


Fig. 2. (colour online) Total and partial densities of states for γ–U at the theoretical equilibrium atomic volume 20.72 Å^3. The Fermi level is set to be zero.

3.4. Optical properties

In performing calculations of optical properties it is common to evaluate the complex dielectric constant and then use the result to express other properties. It is known that the dielectric function is related mainly to the electronic response. The complex dielectric constant $\varepsilon(\omega)$ is given by

$$\varepsilon = \varepsilon_1 + \mathrm{i}\varepsilon_2 = N^2, \tag{6}$$

where ε_1 and ε_2 represent the real part and imaginary part of the complex dielectric constant, respectively, and hence the relation between the real and imaginary parts of the refractive index and dielectric constant is

$$\varepsilon_1 = n^2 - k^2\varepsilon_2 = 2nk. \tag{7}$$

Optical conductivity $\sigma(\omega)$ is another frequently used quantity for expressing optical properties, which is closely related to the dielectric constant as follows:

$$\sigma = \sigma_1 + \mathrm{i}\sigma_2 = -\mathrm{i}\frac{\omega}{4\pi}(\varepsilon - 1). \tag{8}$$

The imaginary part of the dielectric constant is given by

$$\begin{aligned}&\varepsilon_2(q \to O_{\hat{u}}, h\omega)\\ &= \frac{2e^2\pi}{\Omega\varepsilon_0}\sum_{k,v,c}\left|\langle\psi_k^c|u\cdot r|\psi_k^\gamma\rangle\right|^2\delta(E_k^c - E_k^\gamma - E),\end{aligned} \tag{9}$$

where u is the vector determining the polarization of the incident electric field, and $\varepsilon_2(\omega)$ can be thought of as detailing the real transitions between occupied and unoccupied electronic states. Since the dielectric constant describes a causal response, the real and imaginary parts are linked by a Kramers–Kronig transform. This transform is used to obtain the real part of the dielectric function $\varepsilon_1(\omega)$.

The matrix elements of the position operator which are required to describe the electronic transitions in equation (above) may normally be written as matrix elements of the momentum operator allowing straightforward calculation in reciprocal space. The corrected form of the matrix element is

$$\begin{aligned}\langle\psi_k^c|r|_k^\gamma\rangle &= \frac{1}{\mathrm{i}\omega m}\langle\psi_k^c|P|\psi_k^\gamma\rangle\\ &\quad + \frac{1}{\hbar\omega}\langle\psi_k^c(|V_{nl}|, r)\psi_k^\gamma\rangle.\end{aligned} \tag{10}$$

Figures 3 and 4 show the calculated optical conductivities for α–U and γ–U, respectively. The real part of the optical conductivity has an important relationship with the energy band structure. The optical conductivity for bcc uranium is different from that of its ground-state crystal structure (α–U). In Table 3, we have summarized the main peaks and features in the conductivity plot for both phases, and also comparison is made with the experimental features. For α–U, the first maximum appears at 1.48 eV, followed by a shoulder at about 3.45 eV. Then it drops sharply; in a range of 8 eV–15 eV the conductivity is near zero. The second maximum appears at 17.4 eV, followed by another maximum at 19.7 eV. For γ–U, the first maximum is also clearly seen at 1.2 eV, followed by another peak at 3.31 eV. The following two main peaks appear at 8.6 eV and 19.0 eV. We can also see that for γ–U some shoulder peaks appear at 5.6 eV, 11.5 eV and 21.78 eV respectively. From Table 3 it follows that for some peaks (features B and C) the calculated results for α–U accord well with the experimental ones, while for other peaks (feature D and E) of γ–U the calculated results accord well with the experimental results. And for α–U, the feature at 10 eV in the experimental results is not reproduced in Fig. 3, but a different peak appears at 17.4 eV, which is not seen in experimental results. However, since reflectivity reflects a bulk property, it is quite likely that actinide samples, which normally contain some oxygen, will produce a feature somewhere from the oxygen, which can also be seen in the optical spectrum for ThO_2 or UO_2 at 8 eV–11 eV,[26,27] and we suspect that these

same features appear in the metal. The lowest peak in the experimental results is not reproduced in our calculated results for both phases due to some theoretical limits, and also small difference can be seen for features B, C, and E. This may be because the samples are known to have a considerable dependence on surface preparation condition. According to the previous research by Gasche *et al.*,[16] feature E can be assigned to 6p→6d transitions.

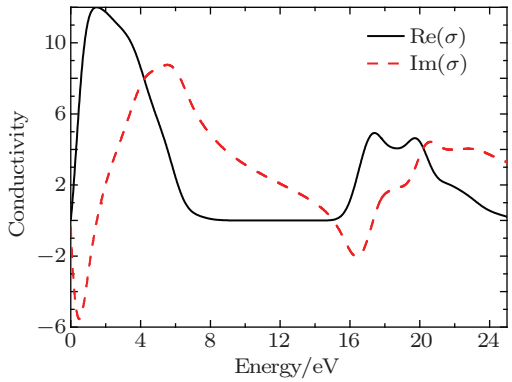


Fig. 3. (colour online) Calculated optical conductivity for α–U in the energy range from 0 to 25 eV.

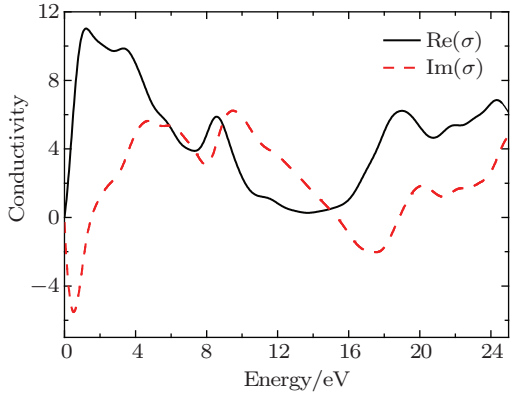


Fig. 4. (colour online) Calculated optical conductivity for γ–U in the energy range from 0 to 25 eV.

Table 3. Summary of theoretical and experimental features for uranium.

Feature	α–U (theory)	γ–U (theory)	Expt. [28]
A	–	–	0.7
B	1.49	1.21	1.4
C	3.45	3.31	3.8
D	17.4	8.56	10
E	19.7	19	19.2

We also calculate dielectric functions for both phases, which can be seen in Figs. 5 and 6. Since dielectric function has a direct relationship with the optical conductivity, and there is a lack of experimental results to be compared with, here we will not give more analyses for the results.

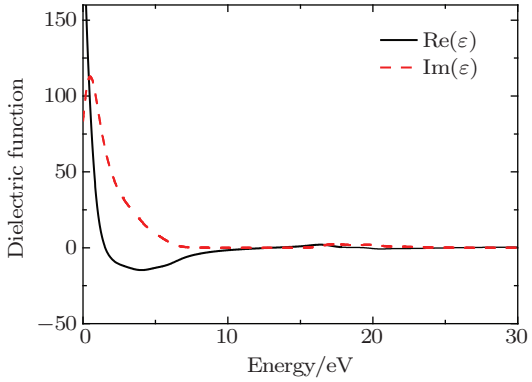


Fig. 5. (colour online) Calculated dielectric function for α–U in an energy range from 0 to 30 eV.

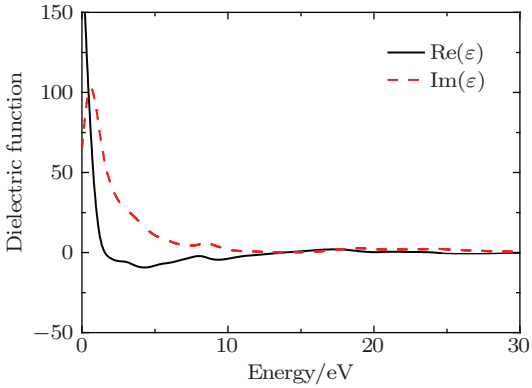


Fig. 6. (colour online) Calculated dielectric function for γ–U in an energy range from 0 to 30 eV.

In our previous work, we have measured the refractive index and extinction coefficient of uranium in a wavelength range of 350 nm–1000 nm. The samples used in our experiments were depleted uranium, which were finely polished before the experiments. The uranium sample was sputtered in vacuum by an argon ion gun first before it was sent to the analysis chamber. Data were obtained from *in-situ* spectroscopic ellipsometry measurement. For more details, please refer to Ref. [8]. In this paper, we also calculate the refractive indices and extinction coefficients for α–U and γ–U. Calculated results are compared with experimental results of our own, and also the available published ones.

From Figs. 7 and 8, we can see that there are also some differences between our experimental results and those given by Siekhaus *et al.*,[7] especially for the extinction coefficients. Since refractive index and extinction coefficient exhibit a bulk property, it is quite likely

that different actinide samples may have different results. For example, in our experiments the uranium samples we used contained some carbon, nitrogen, and oxygen, and they may have had some effect on the results. Also samples are known to have a considerable dependence on surface preparation, and different surface preparation methods may also lead to some differences in results. Overall, the trend is almost the same for both refractive indices and extinction coefficients. Our calculated results for both α–U and γ–U are much larger than the experimental results. There are some reasons for this. Firstly, the experimental samples are not so perfect as the theoretical ones, and may inevitably contain some impurities. Secondly, most of the experiments were done at ambient temperature, while theoretical calculations are at 0 K. Temperature may also be the factor that affects refractive index and extinction coefficient. Thirdly, surface roughness may have obvious effects on the experimental results since ellipsometric spectroscopy technology is sensitive to the surface property. And according to the results in the literature and our experience, we find that the smaller the surface roughness, the larger the optical constant is. So we can make a bold hypothesis that theoretical results should be larger than the experimental ones, which still needs to be further clarified experimentally.

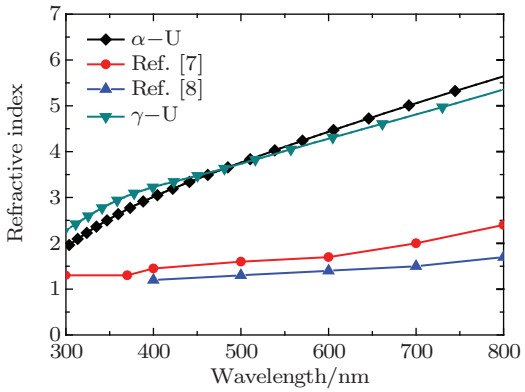


Fig. 7. (colour online) Calculated refractive indices of uranium metal in both α- and γ-phases, and some of the available experimental results are also given here.

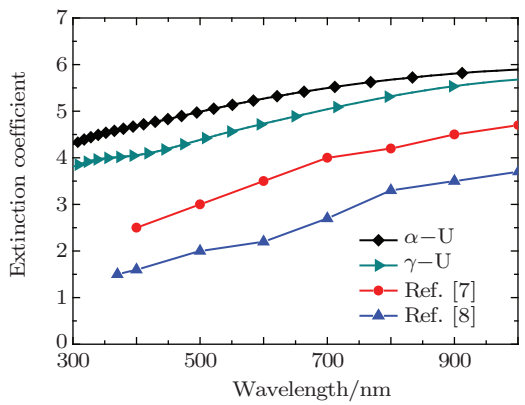


Fig. 8. (colour online) Calculated extinction coefficients of uranium metal in both α- and γ-phases, and some of the available experimental results are also given here.

4. Conclusions

In this paper, we investigated in detail the lattice constants, elastic constants, electronic structures, and optical properties for uranium in both alpha- and gamma-phases using the first-principles method. Comparison is made with experimental results of our own and also the available published ones. The calculated lattice constants and equilibrium atomic volume accord pretty well with the experimental ones. There are some differences in optical conductivity between our calculations and the experimental ones, but the differences are relatively small and acceptable. Refractive indices and extinction coefficients are much larger than experimental results, so further research is needed for clarifying and explaining the discrepancy.

Acknowledgement

We are grateful to Ao Bing-Yun, Gao Tao and Ai Juan-Juan for some instructive suggestions and help.

References

[1] Artioukov I A, Fechtchenko R M and Udovskii A L 2004 *Nucl. Instrum. Methods Phys. Res.* A **372** 517
[2] Artioukov I A, Chefonov O V, Gilev O N, Lipin A V and Oatashev V I 2007 *Nucl. Instrum. Methods Phys. Res.* A **575** 248
[3] Schoenes J 1978 *J. Appl. Phys.* **49** 1463
[4] Meek T T and Roedern B 2009 *Vacuum* **83** 226
[5] Meek T T, Roedern B, Clem P G and Hanrahan R J Jr 2005 *Mater. Lett.* **59** 1085
[6] Faldt A and Nilsson P O 1980 *J. Phys.* F: *Met. Phys.* **10** 2573
[7] Siekhaus W and Nelson A 2005 *Materials Research Society Fall* 2005, Boston, MA, United States. November 28, 2005 through December 2, 2005. UCRL-PROC-217595
[8] Lin L, Lai X, Lü X and Zhang H 2008 *Surf. Interface Anal.* **40** 645
[9] Ritchie A G 1984 *J. Nucl. Mater.* **120** 143
[10] Yang Y P, Feng S, Feng H, Pan X C, Wang Y Q and Wang W Z 2011 *Acta Phys. Sin.* **60** 027802 (in Chinese)
[11] Zeng L G, Liu F M, Zhong W W, Ding P, Cai L G and Zhou C C 2011 *Acta Phys. Sin.* **60** 038203 (in Chinese)
[12] Di G Q 2011 *Acta Phys. Sin.* **60** 038101 (in Chinese)
[13] Ma X F, Wang Y Z and Zhou C Y 2011 *Acta Phys. Sin.* **60** 068102 (in Chinese)
[14] Su R, He J, Chen J S and Guo Y J 2011 *Acta Phys. Sin.* **60** 107101 (in Chinese)

[15] Li D and Zhang X H 2011 *Acta Phys. Sin.* **60** 126102 (in Chinese)
[16] Gasche T, Brooks M S and Johansson B 1996 *Phys. Rev.* B **54** 2446
[17] Wills J M and Eriksson O 1992 *Phys. Rev.* B **45** 13879
[18] Söderlind P, Eriksson O, Johansson B and Wills J M 1994 *Phys. Rev.* B **50** 7291
[19] Jones M D, Boettger J C, Albers R C and Singh D J 2000 *Phys. Rev.* B **61** 4644
[20] Söderlind P, Eriksson O, Johansson B, Wills J M and Boring A M 1995 *Nature* **374** 524
[21] Söderlind P 2002 *Phys. Rev.* B **66** 085113
[22] Taylor C D 2008 *Phys. Rev.* B **77** 094119
[23] Segall M D, Lindan P J D, Probert M J, Pickard C J, Hasnip P J, Clark S J and Payne M C 2002 *J. Phys.: Condens. Matter* **14** 2717
[24] Mattsson A E, Schultz P A, Desjarlais M P, Mattsson T R and Leung K 2005 *Mater. Sci. Eng.* **13** R1
[25] Perdew J P, Burke K and Ernzerhof M 1996 *Phys. Rev. Lett.* **77** 3865
[26] Vanderbilt D 1990 *Phys. Rev.* B **41** 7892
[27] Laasonen K, Pasquarello A, Car R, Lee C and Vanderbilt D 1993 *Phys. Rev.* B **47** 10142
[28] Puddu G 2009 *Eur. Phys. J.* A **39** 335
[29] Crocombette J P, Jollet F, Nga L T and Petit A 2001 *Phys. Rev.* B **64** 104107
[30] Barret C S, Muller M H and Hitterman R H 1963 *Phys. Rev.* B **129** 625
[31] Fisher E S and McSkimin H J 1958 *J. Appl. Phys.* **29** 1473
[32] Veal B W and Lam D J 1994 *Phys. Rev.* B **10** 4902
[33] Schoenes J 1980 *Phys. Rep.* **63** 301
[34] Fäldt P and Nilsson O 1980 *J. Phys.* F **10** 2573